nature mental health

Article

https://doi.org/10.1038/s44220-023-00187-w

Neuroanatomical dimensions in medication-free individuals with major depressive disorder and treatment response to SSRI antidepressant medications or placebo

In the format provided by the authors and unedited

Supplementary materials

Neuroanatomical dimensions in medication-free individuals with major depressive disorder and treatment response to SSRI antidepressant medications or placebo

Cynthia H.Y. Fu, Mathilde Antoniades, Guray Erus, Jose A. Garcia, Yong Fan, Danilo Arnone, Stephen R. Arnott, Taolin Chen, Ki Sueng Choi, Cherise Chin Fatt, Benicio N. Frey, Vibe G. Frokjaer, Melanie Ganz, Beata R. Godlewska, Stefanie Hassel, Keith Ho, Andrew M. McIntosh, Kun Qin, Susan Rotzinger, Matthew D. Sacchet, Jonathan Savitz, Haochang Shou, Ashish Singh, Aleks Stolicyn, Irina Strigo, Stephen C. Strother, Duygu Tosun, Teresa A. Victor, Dongtao Wei, Toby Wise, Roland Zahn, Ian M. Anderson, W. Edward Craighead, J.F. William Deakin, Boadie W. Dunlop, Rebecca Elliott, Qiyong Gong, Ian H. Gotlib, Catherine Harmer, Sidney H. Kennedy, Gitte M. Knudsen, Helen S. Mayberg, Martin P. Paulus, Jiang Qiu, Madhukar H. Trivedi, Heather C. Whalley, Chao-Gan Yan, Allan H. Young, Christos Davatzikos

Table of Contents

Supplementary Method 1. Description of main datasets in this study

Full descriptions of the datasets are available in: Fu CHY, Erus G, Fan Y, Antoniades M, et al., AI-based dimensional neuroimaging system for characterizing heterogeneity in brain structure and function in major depressive disorder: COORDINATE-MDD consortium design and rationale. BMC Psychiatry. Jan 23 2023;23(1):59. doi:10.1186/s12888-022-04509-7.

Main datasets in this study are as follows:

1. Canadian Biomarker Integration Network in Depression (CAN-BIND) is a national depression program with recruitment from 7 centers (MacQueen et al., 2019). Treatment protocol is 8-week trial with SSRI antidepressant (escitalopram) followed by an augmentation trial if there is poor treatment response (i.e., less than 50% improvement in depressive symptoms). MRI scans have been acquired at baseline, weeks 2 and 8 in both MDD and healthy participants.

2. Establishing Moderators and Biosignatures of Antidepressant Response in Clinical Care (EMBARC) is a multisite, randomized, placebo-controlled clinical trial with recruitment from 4 centers (Trivedi et al., 2016). Treatment protocol is an 8-week double-blind randomized allocation to SSRI (escitalopram) or placebo, with double-blind cross over switch to another antidepressant if there is poor treatment response. MRI scans have been acquired in MDD and healthy participants at baseline.

3. Huaxi MR Research Center at Sichuan University (SCU) cohort consists of medication-naïve first episode MDD and matched healthy participants (Qiu et al., 2018; Zhao et al., 2020; Zhao et al., 2021).

4. King's College London cohort consists of 4 studies (Green et al., 2012; Nouretdinov et al., 2011; Sankar et al., 2016; Wise et al., 2017, 2018). MRI scans have been acquired in MDD and healthy participants, and the treatment study is an 8-week selective serotonin and norepinephrine reuptake inhibitor (SNRI) antidepressant (duloxetine) with MRI scans at baseline, weeks 2 and 8 in both MDD and healthy participants.

5. Laureate Institute for Brain Research (LIBR) cohort consists of MRI data in first episode and recurrent MDD and matched healthy controls from 2 studies (Ford et al., 2019; Misaki et al., 2016; Zheng et al., 2021).

6. Manchester cohort consists of 3 studies (Arnone et al., 2012, 2013; Dutta et al., 2019). All participants have a baseline MRI scan, and the treatment study is 8-week SSRI (citalopram) with MRI scans at baseline and week 8 (Arnone et al., 2012).

7. Oxford cohort consists of 6-week SSRI (escitalopram) treatment with MRI scans at baseline and week 6 (Godlewska et al., 2014, 2018).

8. Predictors of Remission in Depression to Individual and Combined Treatments (PReDICT) study is a 12-week randomized clinical trial of treatment-naïve MDD participants with 3 treatment arms: SSRI (escitalopram), SNRI (duloxetine), or CBT, with an augmentation trial if is there no remission. MRI scans were acquired at baseline (Dunlop et al., 2012).

9. Southwest University (SWU) cohort consists of a community-based recruitment which includes first episode and recurrent MDD and healthy control participant (Liu et al., 2017, 2021; Hu et al., 2021).

10. Stanford (SNAP) cohort consists of first episode and recurrent MDD and healthy participants (Sacchet & Gotlib, 2017; Sacchet et al., 2019).

11. Stratifying Resilience and Depression Longitudinally (STRADL) is a community-based cohort from the Generation Scotland Scottish Family Health Study with detailed clinical, cognitive and neuroimaging assessments (Habota et al., 2019). Single session MRI scans were acquired.

All patients are adults with a primary diagnosis of MDD that is first episode or recurrent, in a current episode of a moderate to severe severity, that is non-psychotic. MDD diagnosis was based on DSM-IV (SCU, Manchester, Oxford) or DSM-IV-TR (CAN-BIND, EMBARC, KCL, LIBR, Stanford SNAP, STRADL) using the Structured Clinical Interview for DSM (SCID) (EMBARC, SCU, KCL, Manchester, Oxford, Stanford SNAP, STRADL) or Mini International Neuropsychiatric Interview (MINI) (CAN-BIND, KCL).

Depressive severity was measured with standardized clinician-rated scales: 17-item Hamilton Rating Scale for Depression (HRSD, (Hamilton, 1960) (EMBARC, SCU, KCL, Oxford, PREDICT, Stanford SNAP), Montgomery-Åsberg Depression Rating Scale (MADRS) (Montgomery & Asberg, 1979)(CAN-BIND, LIBR, Manchester), or Quick Inventory of Depressive Symptomatology (QIDS) (Rush et al., 2003; Trivedi et al., 2004)(STRADL). The rating scales show high correlation in summed scores and percentage score improvements (Leucht et al., 2018; Rush et al., 2003; Uher et al., 2008).

Supplementary Method 2. Estimation of years of education

Wherever raw text was provided, it was converted into years of education. Unless indicated we assumed that the degree was completed and allocated the maximum number of years associated with completing the degree or diploma. The calculation assumed that participants started school at the age of 5.

Raw text	Years of education attributed
No education	0
Primary school	6
Middle school	8
Some high school (10th, 11th)	11
High school	12
GED or alternative credential	12
12th grade, no diploma	12
Some college credit, but less than 1 year of college credit	12.5
1 or more years of college credit, no degree	13
Some college, no degree	13
Some college	14
Tech school	14
Associate's degree (for example: AA, AS)	14
Trade school	14
College and above	16
Four-year college	16
Junior College	16
Bachelor's degree	16
Some graduate school	17
Grad or Prof Degree	18
Master's degree	18
Doctorate	23

Supplementary Results 1. Comparison of estimated prior medication status across HYDRA dimensions

In order to compare medication exposure across HYDRA dimensions we used a Chi-squared test to determine if the dimensions differed in the number of MDD participants with first episode or recurrent depression. In Dimension 1, 201 participants had recurrent MDD and 89 participants had first episode MDD. In D2, 222 patients had recurrent MDD and 173 had first episode MDD. The Chi-squared test showed a significant difference between the dimensions (X^2=11.6, p=0.0007).

Supplementary Results 2. Interaction between HYDRA dimensions and treatment outcomes whilst controlling for medication and education

The interaction between HYDRA dimension and treatment group was examined using a linear regression model with the percentage change in the clinician-rated depressive symptom scale (continuous) as the outcome variable and HYDRA dimension (categorical, 2 groups) and treatment group (categorical, 2 groups: SSRI and placebo) as the independent variables whilst controlling for age, sex, site, years of education (as a proxy for IQ) and medication status (using first-episode or recurrent MDD as a proxy measure).

Treatment with SSRI medications was associated with a significantly greater improvement in depressive symptoms across both D1 and D2 (β=34.5, 95% CI (7.2 to 61.7), p=0.01).

The Dimension by treatment interaction remained significant after controlling for age, sex, site, medication status and years of education (β=-19.1, 95% CI (-36.4 to -1.8), p=0.03).

In order to examine whether the interaction between Dimensions and treatment group differed according to SSRI medication, we performed a second linear regression with the treatment group variable including all four treatment categories (SSRI sertraline, SSRI escitalopram, SSRI citalopram and placebo) instead of a binary category (SSRI medications and placebo). The covariates of this linear model included age, sex, site, medication status and years of education. There was a significant interaction between treatment with sertraline and HYDRA dimension (β=-24.1, 95% CI (-43.8 to -4.4), p=0.02). The interaction was not significant for escitalopram (β=-12.1, 95% CI (-33.8 to 9.6), p=0.27) or citalopram ($\beta=5.9\times10^{-15}$, 95% CI (-1.3×10^{-15} to 1.3×10^{-14}), p=0.11).

Supplementary Figure 1

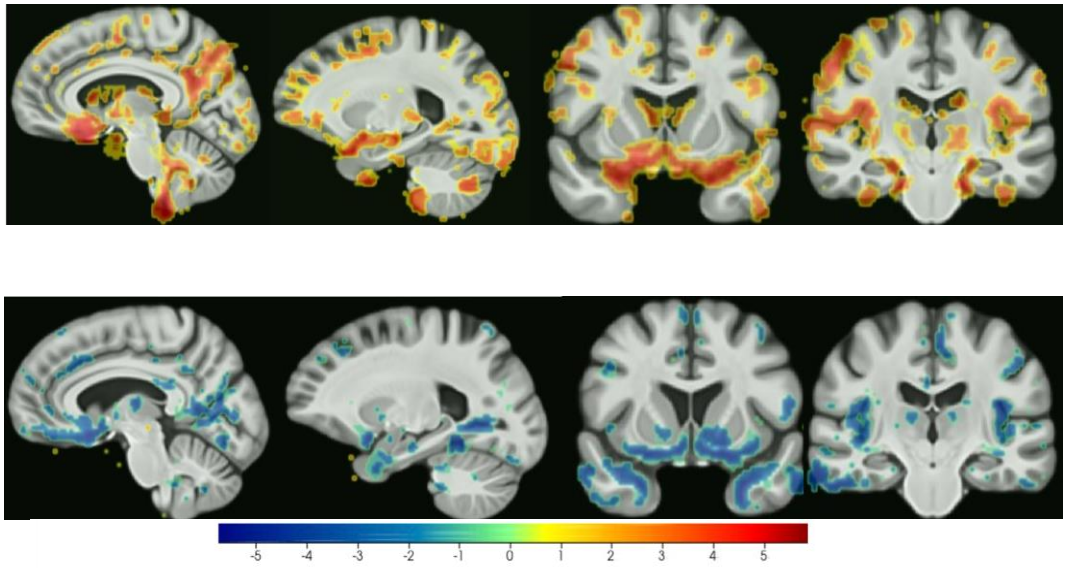

Additional coronal and sagittal views for dimensions 1 and 2 (top and bottom rows respectively), indicating areas with significant differences from controls. Colour represents direction and strength of group differences as indicated by the colour bar.

Supplementary Figure 2

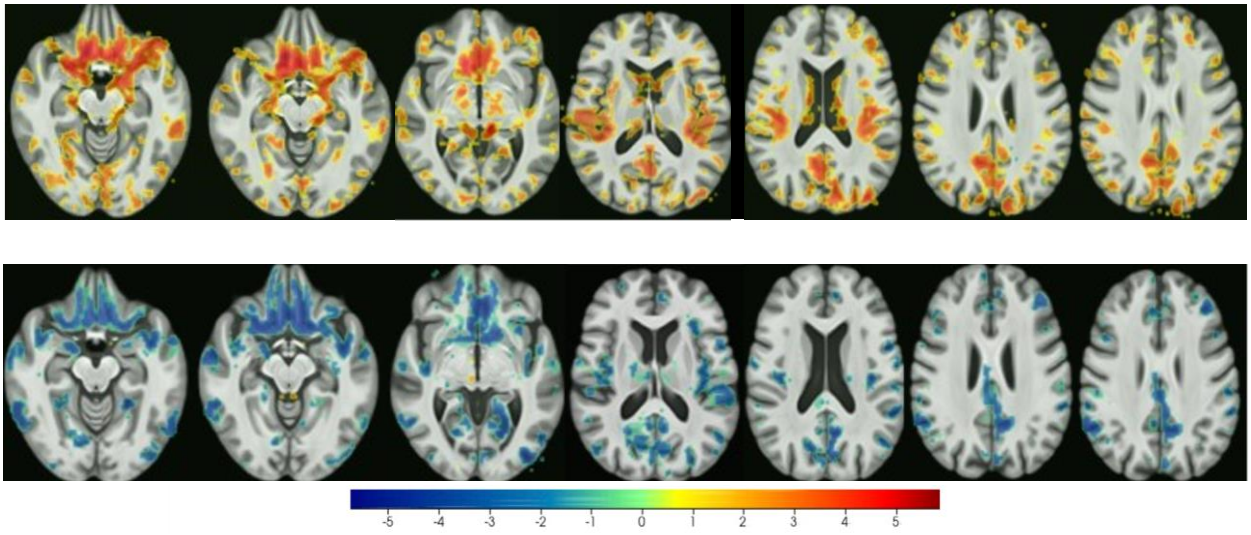

Additional transverse views for dimensions 1 and 2 (top and bottom rows respectively), indicating areas with significant differences from controls. Colour represents direction and strength of group differences as indicated by the colour bar.

Supplementary Figure 3

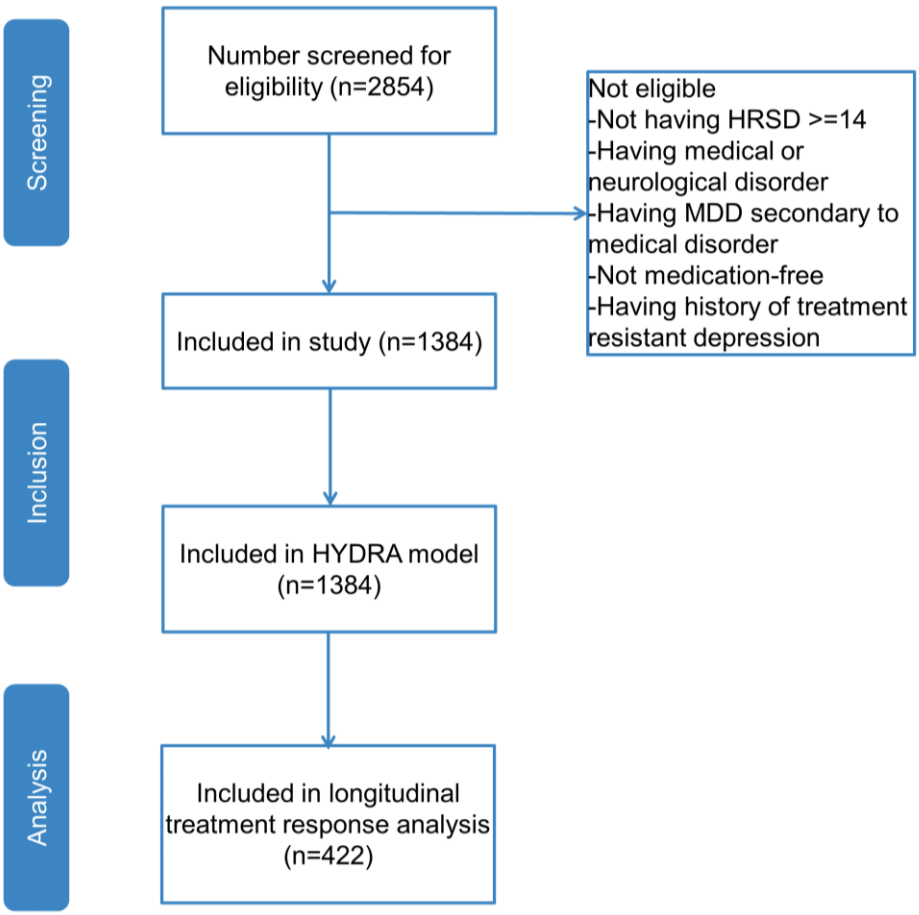

Supplementary Figure 3. Flow diagram of the screening process to include subjects in the final analyses.

Supplementary Figure 4

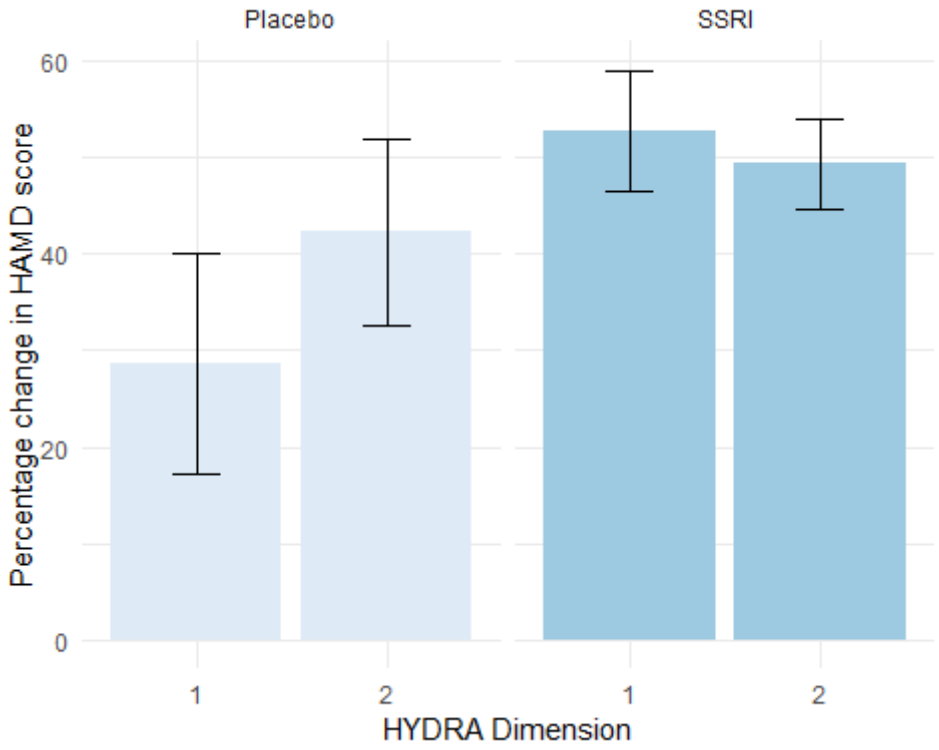

Supplementary Figure 4. Difference in percentage change in HAMD scores across HYDRA Dimensions (D1 (n=169) and D2 (n=253), n=422) and binary treatment groups following treatment with SSRI medications (n=313) and placebo (n=109). The sample consists of all five cohorts including PReDICT. Data are presented using a bar plot as mean values and 95th percentile error bars. The asterisks (*) indicate significant differences between the two subgroups using linear regression model (two-sided $P < 0.05$).

Supplementary Figure 5

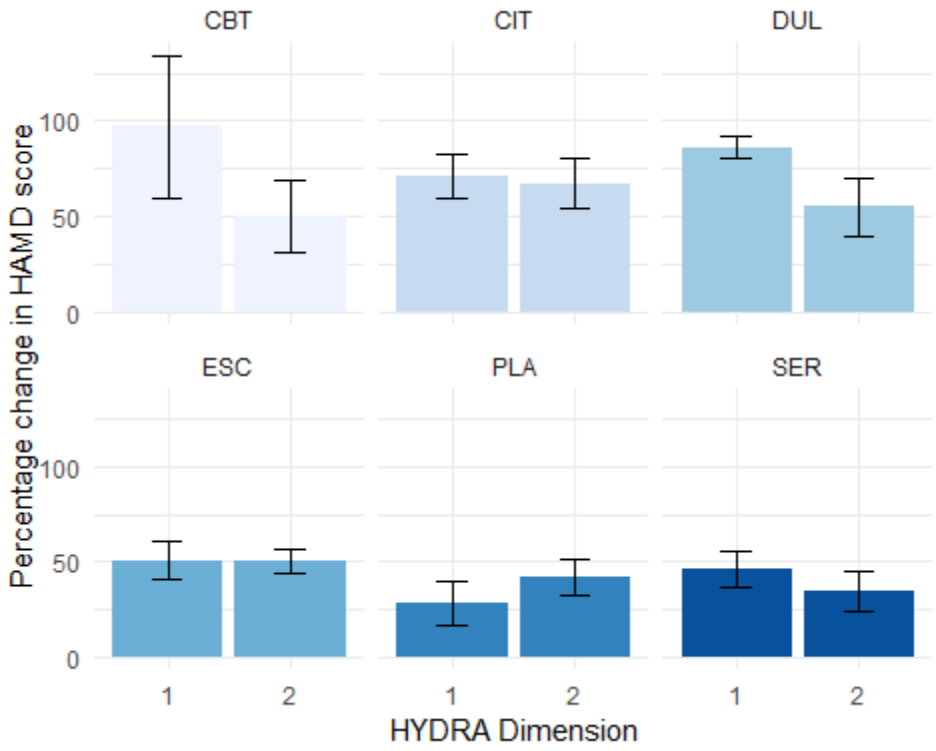

Supplementary Figure 5. Difference in percentage change in HAMD scores across HYDRA Dimensions (D1 (n=164) and D2 (n=195), n=359) and 6 different treatment groups following treatment with cognitive behavioral therapy (CBT, N=19), placebo medication (PLA, N=109), citalopram medication (CIT, n=36), duloxetine medication (DUL, N=20), escitalopram medication (ESC, N=140), sertraline medication (SER, n=98). The sample consists of all five cohorts including PReDICT. Data are presented using a bar plot as mean values and 95th percentile error bars. The asterisks (*) indicate significant differences between the two subgroups using linear regression model (two-sided $P < 0.05$).

Supplementary Table 1. Scanner protocols

	CAN-BIND	EMBARC	HMRRC	Manchester	LIBR	Oxford	PReDICT	Stanford	STRADL
Scanner model	GE 3T Signa HDxt	All 3T: GE Signa HDx; Siemens TrioTim, Philips Ingenia	3T Siemens Trio	Philips Intera 1.5T	GE 3T Discovery MR750	3T Siemens TIM Trio	3T Siemens Magnetom TIM Trio	1.5T GE Signa Excite	3T Philips Achieva TX; Siemens 3T Prisma fit
T1 Resolution (mm^3)	1x1x1	1x1x1	0.94x0.94x1	0.875x0.875x1	0.9375x0.9375x0.9	1x1x1	1x1x1	0.86x0.86	1x1x1
TR/TE (ms)	7.5/2.86	5.9-8.2/2.4-3.7	1900/2.26	8.99/4.2	5.0/2.0	20040/ 4.68	2300/2-4	8.3-10.1/ 1.7-3.0	8.2/3.8
Number of volumes	176	160	176	160	120			116	160

Supplementary Table 2. Demographic information for healthy control participants by site

Site	Sample size	Age (mean)	F/M (n)	Years of education (mean)	HAMD	MADRS	QIDS
CAN-BIND	23	33.3	12/11	15.1		0.6	
EMBARC	39	37.1	24/15	15.1	0.6		
HMRRC	139	30.9	71/68	12.9	NA		
KCL-Blame	46	33.4	29/17	17.3		0.7	
KCL-BUD	20	30.1	18/2	17.5		1.0	
LIBR-B	81	30.5	44/37	15.0	1.9		
LIBR-S	60	32.0	39/21	14.6	1.8		
Manchester	30	33.3	21/9	NA		0.1	
Oxford	31	30.3	18/13	NA	0.4		
PReDICT	0	NA	NA	NA			
Stanford	50	32.6	33/17	16.0	2.0		
STRADL	180	56.8	95/85	16.0			2.7
Total	699	38.4	404/295	15.3	1.5	0.6	2.7

Age was not part of our inclusion/exclusion criteria so it was just happenstance that the groups have different age ranges. The number of controls by age above 65 is as follows:

65	N=6
66	N=4
67	N=2
68	N=4
69	N=1
70	N=2
71	N=4
72	N=1

Supplementary Table 3. Demographic information for MDD participants by site

Site	Sample size	Dimension 1/2	Age (mean)	F/M (n)	FE/RC	Years of education (mean)	Age of onset (mean, sd)	HAMD	MADRS	QIDS
CAN-BIND	92	27/65	36.0	61/31	14/49	13.9	22.0 (10.9)		29.7	
EMBARC	257	134/123	36.6	166/91	1/253	15.1		19.5		
HMRRC	111	53/58	31.7	65/46	81/0	13.2		25.2		
KCL-BUD	20	10/10	29.6	18/2		15.1	22.8 (7.8)		27.3	
LIBR-B	32	14/18	35.3	21/11		14.0		18.5		
LIBR-S	22	12/10	35.2	15/7		14.0		19.6		
Manchester	40	19/21	36.4	27/13	3/37		22.0 (8.1)		27.3	
Oxford	39	14/25	29.9	24/15	25/14		25.4 (9.1)	22.7		
PReDICT	63	5/58	39.3	36/27		15.0	29.7 (12.2)	18.3		
Stanford	8	2/6	34.0	5/3	4/2	15.0		17.5		
STRADL	1	0/1	59.0	1/0		16.0				16
Total	685	290/395	35.3	439/246	128/355	14.5	24.5 (10.8)	21.2	29.0	16

Supplementary Table 4. List of structural MUSE regions of interest used in the HYDRA model

ROI index	ROI Name	ROI Resolution
4	3rd Ventricle	Single
11	4th Ventricle	Single
23	Right Accumbens Area	Single
30	Left Accumbens Area	Single
31	Right Amygdala	Single
32	Left Amygdala	Single
35	Brain Stem	Single
36	Right Caudate	Single
37	Left Caudate	Single
38	Right Cerebellum Exterior	Single
39	Left Cerebellum Exterior	Single
40	Right Cerebellum White Matter	Single
41	Left Cerebellum White Matter	Single
47	Right Hippocampus	Single
48	Left Hippocampus	Single
49	Right Inferior Lateral Ventricle	Single
50	Left Inferior Lateral Ventricle	Single
51	Right Lateral Ventricle	Single
52	Left Lateral Ventricle	Single
55	Right Pallidum	Single
56	Left Pallidum	Single
57	Right Putamen	Single
58	Left Putamen	Single
59	Right Thalamus Proper	Single
60	Left Thalamus Proper	Single
61	Right Ventral DC	Single
62	Left Ventral DC	Single
71	Cerebellar Vermal Lobules I-V	Single
72	Cerebellar Vermal Lobules VI-VII	Single
73	Cerebellar Vermal Lobules VIII-X	Single
75	Left Basal Forebrain	Single
76	Right Basal Forebrain	Single
81	Frontal lobe white matter right	Single
82	Frontal lobe white matter left	Single
83	Occipital lobe white matter right	Single
84	Occipital lobe white matter left	Single
85	Parietal lobe white matter right	Single
86	Parietal lobe white matter left	Single
87	Temporal lobe white matter right	Single

88	Temporal lobe white matter left	Single
89	Right fornix	Single
90	Left fornix	Single
91	Anterior limb of internal capsule right	Single
92	Anterior limb of internal capsule left	Single
93	Posterior limb of internal capsule inc. cerebral peduncle right	Single
94	Posterior limb of internal capsule inc. cerebral peduncle left	Single
95	Corpus callosum	Single
100	Right anterior cingulate gyrus	Single
101	Left anterior cingulate gyrus	Single
102	Right anterior insula	Single
103	Left anterior insula	Single
104	Right anterior orbital gyrus	Single
105	Left anterior orbital gyrus	Single
106	Right angular gyrus	Single
107	Left angular gyrus	Single
108	Right calcarine cortex	Single
109	Left calcarine cortex	Single
112	Right central operculum	Single
113	Left central operculum	Single
114	Right cuneus	Single
115	Left cuneus	Single
116	Right entorhinal area	Single
117	Left entorhinal area	Single
118	Right frontal operculum	Single
119	Left frontal operculum	Single
120	Right frontal pole	Single
121	Left frontal pole	Single
122	Right fusiform gyrus	Single
123	Left fusiform gyrus	Single
124	Right gyrus rectus	Single
125	Left gyrus rectus	Single
128	Right inferior occipital gyrus	Single
129	Left inferior occipital gyrus	Single
132	Right inferior temporal gyrus	Single
133	Left inferior temporal gyrus	Single
134	Right lingual gyrus	Single
135	Left lingual gyrus	Single
136	Right lateral orbital gyrus	Single
137	Left lateral orbital gyrus	Single
138	Right middle cingulate gyrus	Single
139	Left middle cingulate gyrus	Single
140	Right medial frontal cortex	Single

141	Left medial frontal cortex	Single
142	Right middle frontal gyrus	Single
143	Left middle frontal gyrus	Single
144	Right middle occipital gyrus	Single
145	Left middle occipital gyrus	Single
146	Right medial orbital gyrus	Single
147	Left medial orbital gyrus	Single
148	Right postcentral gyrus medial segment	Single
149	Left postcentral gyrus medial segment	Single
150	Right precentral gyrus medial segment	Single
151	Left precentral gyrus medial segment	Single
152	Right superior frontal gyrus medial segment	Single
153	Left superior frontal gyrus medial segment	Single
154	Right middle temporal gyrus	Single
155	Left middle temporal gyrus	Single
156	Right occipital pole	Single
157	Left occipital pole	Single
160	Right occipital fusiform gyrus	Single
161	Left occipital fusiform gyrus	Single
162	Right opercular part of the inferior frontal gyrus	Single
163	Left opercular part of the inferior frontal gyrus	Single
164	Right orbital part of the inferior frontal gyrus	Single
165	Left orbital part of the inferior frontal gyrus	Single
166	Right posterior cingulate gyrus	Single
167	Left posterior cingulate gyrus	Single
168	Right precuneus	Single
169	Left precuneus	Single
170	Right parahippocampal gyrus	Single
171	Left parahippocampal gyrus	Single
172	Right posterior insula	Single
173	Left posterior insula	Single
174	Right parietal operculum	Single
175	Left parietal operculum	Single
176	Right postcentral gyrus	Single
177	Left postcentral gyrus	Single
178	Right posterior orbital gyrus	Single
179	Left posterior orbital gyrus	Single
180	Right planum polare	Single
181	Left planum polare	Single
182	Right precentral gyrus	Single
183	Left precentral gyrus	Single
184	Right planum temporale	Single
185	Left planum temporale	Single

186	Right subcallosal area	Single
187	Left subcallosal area	Single
190	Right superior frontal gyrus	Single
191	Left superior frontal gyrus	Single
192	Right supplementary motor cortex	Single
193	Left supplementary motor cortex	Single
194	Right supramarginal gyrus	Single
195	Left supramarginal gyrus	Single
196	Right superior occipital gyrus	Single
197	Left superior occipital gyrus	Single
198	Right superior parietal lobule	Single
199	Left superior parietal lobule	Single
200	Right superior temporal gyrus	Single
201	Left superior temporal gyrus	Single
202	Right temporal pole	Single
203	Left temporal pole	Single
204	Right triangular part of the inferior frontal gyrus	Single
205	Left triangular part of the inferior frontal gyrus	Single
206	Right transverse temporal gyrus	Single
207	Left transverse temporal gyrus	Single
301	FRONTAL_INFERIOR_GM	Composite
302	FRONTAL_INSULAR_GM	Composite
303	FRONTAL_LATERAL_GM	Composite
304	FRONTAL_MEDIAL_GM	Composite
305	FRONTAL_OPERCULAR_GM	Composite
306	LIMBIC_CINGULATE_GM	Composite
307	LIMBIC_MEDIALTEMPORAL_GM	Composite
308	OCCIPITAL_INFERIOR_GM	Composite
309	OCCIPITAL_LATERAL_GM	Composite
310	OCCIPITAL_MEDIAL_GM	Composite
311	PARIETAL_LATERAL_GM	Composite
312	PARIETAL_MEDIAL_GM	Composite
313	TEMPORAL_INFERIOR_GM	Composite
314	TEMPORAL_LATERAL_GM	Composite
315	TEMPORAL_SUPRATEMPORAL_GM	Composite
316	FRONTAL_INFERIOR_GM_L	Composite
317	FRONTAL_INSULAR_GM_L	Composite
318	FRONTAL_LATERAL_GM_L	Composite
319	FRONTAL_MEDIAL_GM_L	Composite
320	FRONTAL_OPERCULAR_GM_L	Composite
321	LIMBIC_CINGULATE_GM_L	Composite
322	LIMBIC_MEDIALTEMPORAL_GM_L	Composite
323	OCCIPITAL_INFERIOR_GM_L	Composite

324	OCCIPITAL_LATERAL_GM_L	Composite
325	OCCIPITAL_MEDIAL_GM_L	Composite
326	PARIETAL_LATERAL_GM_L	Composite
327	PARIETAL_MEDIAL_GM_L	Composite
328	TEMPORAL_INFERIOR_GM_L	Composite
329	TEMPORAL_LATERAL_GM_L	Composite
330	TEMPORAL_SUPRATEMPORAL_GM_L	Composite
331	FRONTAL_INFERIOR_GM_R	Composite
332	FRONTAL_INSULAR_GM_R	Composite
333	FRONTAL_LATERAL_GM_R	Composite
334	FRONTAL_MEDIAL_GM_R	Composite
335	FRONTAL_OPERCULAR_GM_R	Composite
336	LIMBIC_CINGULATE_GM_R	Composite
337	LIMBIC_MEDIALTEMPORAL_GM_R	Composite
338	OCCIPITAL_INFERIOR_GM_R	Composite
339	OCCIPITAL_LATERAL_GM_R	Composite
340	OCCIPITAL_MEDIAL_GM_R	Composite
341	PARIETAL_LATERAL_GM_R	Composite
342	PARIETAL_MEDIAL_GM_R	Composite
343	TEMPORAL_INFERIOR_GM_R	Composite
344	TEMPORAL_LATERAL_GM_R	Composite
345	TEMPORAL_SUPRATEMPORAL_GM_R	Composite
401	BASAL_GANGLIA	Composite
402	DEEP_GM	Composite
403	DEEP_WM	Composite
404	FRONTAL_GM	Composite
405	FRONTAL_WM	Composite
406	LIMBIC_GM	Composite
407	OCCIPITAL_GM	Composite
408	OCCIPITAL_WM	Composite
409	PARIETAL_GM	Composite
410	PARIETAL_WM	Composite
411	TEMPORAL_GM	Composite
412	TEMPORAL_WM	Composite
413	BASAL_GANGLIA_L	Composite
414	DEEP_GM_L	Composite
415	DEEP_WM_L	Composite
416	FRONTAL_GM_L	Composite
417	FRONTAL_WM_L	Composite
418	LIMBIC_GM_L	Composite
419	OCCIPITAL_GM_L	Composite
420	OCCIPITAL_WM_L	Composite
421	PARIETAL_GM_L	Composite

422	PARIETAL_WM_L	Composite
423	TEMPORAL_GM_L	Composite
424	TEMPORAL_WM_L	Composite
425	BASAL_GANGLIA_R	Composite
426	DEEP_GM_R	Composite
427	DEEP_WM_R	Composite
428	FRONTAL_GM_R	Composite
429	FRONTAL_WM_R	Composite
430	LIMBIC_GM_R	Composite
431	OCCIPITAL_GM_R	Composite
432	OCCIPITAL_WM_R	Composite
433	PARIETAL_GM_R	Composite
434	PARIETAL_WM_R	Composite
435	TEMPORAL_GM_R	Composite
436	TEMPORAL_WM_R	Composite
501	CORPUS_CALLOSUM	Composite
502	CEREBELLUM	Composite
503	DEEP_WM_GM	Composite
504	FRONTAL	Composite
505	LIMBIC	Composite
506	OCCIPITAL	Composite
507	PARIETAL	Composite
508	TEMPORAL	Composite
509	VENTRICLE	Composite
510	CEREBELLUM_L	Composite
511	DEEP_WM_GM_L	Composite
512	FRONTAL_L	Composite
513	LIMBIC_L	Composite
514	OCCIPITAL_L	Composite
515	PARIETAL_L	Composite
516	TEMPORAL_L	Composite
517	VENTRICLE_L	Composite
518	CEREBELLUM_R	Composite
519	DEEP_WM_GM_R	Composite
520	FRONTAL_R	Composite
521	LIMBIC_R	Composite
522	OCCIPITAL_R	Composite
523	PARIETAL_R	Composite
524	TEMPORAL_R	Composite
525	VENTRICLE_R	Composite
601	GM	Composite
604	WM	Composite
606	GM_L	Composite

607	WM_L	Composite
613	GM_R	Composite
614	WM_R	Composite
701	TOTALBRAIN	Composite
702	ICV	Composite

Supplementary Table 5. Results from linear model used to examine regional volumetric differences between patients with first-episode depression (n=255) and healthy controls (n=558) with age, sex and years of education as covariates. Two-sided p values are presented along with FDR-corrected p values to account for multiple comparisons. Bold lettering indicates volume differences that are significant after FDR correction.

ROI	t value	p value	FDR-corrected p value
Third Ventricle	-1.07	0.29	0.40
Fourth Ventricle	-0.36	0.72	0.82
Right Accumbens Area	-0.75	0.45	0.57
Left Accumbens Area	-0.99	0.32	0.43
Right Amygdala	-1.87	0.06	0.12
Left Amygdala	0.19	0.85	0.90
Brain Stem	-0.53	0.60	0.71
Right Caudate	-0.57	0.57	0.68
Left Caudate	-0.80	0.42	0.53
Right Cerebellum Exterior	-2.15	0.03	0.07
Left Cerebellum Exterior	-2.36	0.02	0.05
Right Cerebellum White Matter	0.12	0.90	0.94
Left Cerebellum White Matter	0.05	0.96	0.97
Right Hippocampus	-0.29	0.77	0.85
Left Hippocampus	-0.86	0.39	0.51
Right Inferior Lateral Ventricle	-0.08	0.94	0.96
Left Inferior Lateral Ventricle	-0.04	0.97	0.98
Right Lateral Ventricle	-1.29	0.20	0.28
Left Lateral Ventricle	-0.66	0.51	0.63
Right Pallidum	-0.17	0.87	0.92
Left Pallidum	-0.01	0.99	0.99
Right Putamen	0.69	0.49	0.61
Left Putamen	0.29	0.77	0.85
Right Thalamus Proper	0.84	0.40	0.51
Left Thalamus Proper	-0.26	0.79	0.86
Right Ventral DC	-2.79	0.01	**0.02**
Left Ventral DC	-2.57	0.01	**0.03**
Cerebellar Vermal Lobules I-V	-3.17	0.002	**0.01**
Cerebellar Vermal Lobules VI-VII	0.98	0.33	0.44
Cerebellar Vermal Lobules VIII-X	-1.69	0.09	0.15
Left Basal Forebrain	-5.90	5.93E-9	**2.15E-7**
Right Basal Forebrain	-6.22	8.96E-10	**6.50E-8**
Right frontal lobe WM	-3.03	0.003	**0.01**
Left frontal lobe WM	-2.59	0.01	**0.03**

Right occipital lobe WM	-4.12	0.00004	**0.0004**
Left occipital lobe WM	-2.74	0.01	**0.02**
Right parietal lobe WM	-3.57	0.0004	**0.003**
Left parietal lobe WM	-3.83	0.0001	**0.001**
Right temporal lobe WM	-2.00	0.05	0.09
Left temporal lobe WM	-2.22	0.03	0.06
Right fornix	-0.30	0.76	0.85
Left fornix	-1.70	0.09	0.15
Right anterior limb of internal capsule	-0.39	0.70	0.80
Left anterior limb of internal capsule	0.89	0.37	0.49
Right posterior limb of internal capsule inc. cerebral peduncle	-3.02	0.003	**0.01**
Left posterior limb of internal capsule inc. cerebral peduncle	-2.66	0.01	**0.03**
Corpus callosum	-1.55	0.12	0.19
Right anterior cingulate gyrus	-4.55	6.38E-6	**0.0001**
Left anterior cingulate gyrus	-2.88	0.004	**0.02**
Right anterior insula	-2.35	0.02	0.05
Left anterior insula	-2.46	0.01	**0.04**
Right anterior orbital gyrus	-3.19	0.001	**0.01**
Left anterior orbital gyrus	-1.02	0.31	0.42
Right angular gyrus	-4.44	0.00001	**0.0001**
Left angular gyrus	-1.84	0.07	0.12
Right calcarine cortex	0.05	0.96	0.97
Left calcarine cortex	2.26	0.02	0.06
Right central operculum	-5.81	9.94E-9	**2.88E-7**
Left central operculum	-3.27	0.001	**0.01**
Right cuneus	-1.19	0.23	0.33
Left cuneus	-2.32	0.02	0.05
Right entorhinal area	-1.71	0.09	0.15
Left entorhinal area	-1.66	0.10	0.16
Right frontal operculum	-1.33	0.19	0.27
Left frontal operculum	-3.07	0.002	**0.01**
Right frontal pole	-4.59	5.23E-6	**0.0001**
Left frontal pole	-6.08	2.11E-9	**1.02E-7**
Right fusiform gyrus	-1.55	0.12	0.19
Left fusiform gyrus	-2.00	0.05	0.09
Right gyrus rectus	-4.99	7.74E-7	**0.00002**
Left gyrus rectus	-4.11	0.00004	**0.0004**
Right inferior occipital gyrus	1.83	0.07	0.12
Left inferior occipital gyrus	2.23	0.03	0.06
Right inferior temporal gyrus	-4.11	0.00005	**0.0004**

Left inferior temporal gyrus	-3.03	0.003	**0.01**
Right lingual gyrus	-2.41	0.02	**0.04**
Left lingual gyrus	-3.18	0.002	**0.01**
Right lateral orbital gyrus	-0.32	0.75	0.84
Left lateral orbital gyrus	-3.20	0.001	**0.01**
Right middle cingulate gyrus	-1.75	0.08	0.14
Left middle cingulate gyrus	-1.63	0.10	0.17
Right medial frontal cortex	-4.45	9.96E-6	**0.0001**
Left medial frontal cortex	-2.28	0.02	0.05
Right middle frontal gyrus	-3.13	0.002	**0.01**
Left middle frontal gyrus	-3.33	0.001	**0.01**
Right middle occipital gyrus	-2.61	0.01	**0.03**
Left middle occipital gyrus	-1.92	0.06	0.11
Right medial orbital gyrus	-3.38	0.001	**0.01**
Left medial orbital gyrus	0.20	0.84	0.90
Right postcentral gyrus medial segment	-1.77	0.08	0.14
Left postcentral gyrus medial segment	-4.13	0.00004	**0.0004**
Right precentral gyrus medial segment	-0.51	0.61	0.72
Left precentral gyrus medial segment	1.13	0.26	0.37
Right superior frontal gyrus medial segment	-1.02	0.31	0.42
Left superior frontal gyrus medial segment	-2.66	0.01	0.03
Right middle temporal gyrus	-2.29	0.02	0.05
Left middle temporal gyrus	-2.28	0.02	0.05
Right occipital pole	-2.36	0.02	0.05
Left occipital pole	-1.42	0.16	0.24
Right occipital fusiform gyrus	-0.65	0.52	0.63
Left occipital fusiform gyrus	-2.04	0.04	0.08
Right opercular part of the inferior frontal gyrus	-1.47	0.14	0.22
Left opercular part of the inferior frontal gyrus	-2.15	0.03	0.07
Right orbital part of the inferior frontal gyrus	-0.25	0.80	0.87
Left orbital part of the inferior frontal gyrus	0.86	0.39	0.51
Right posterior cingulate gyrus	-1.90	0.06	0.11
Left posterior cingulate gyrus	-0.63	0.53	0.64
Right precuneus	-1.41	0.16	0.24
Left precuneus	-3.10	0.002	**0.01**
Right parahippocampal gyrus	-1.70	0.09	0.15
Left parahippocampal gyrus	-1.67	0.10	0.16
Right posterior insula	-2.50	0.01	**0.04**
Left posterior insula	-3.66	0.0003	**0.002**
Right parietal operculum	2.34	0.02	0.05
Left parietal operculum	-1.31	0.19	0.27
Right postcentral gyrus	-3.31	0.001	**0.01**

Left postcentral gyrus	-1.94	0.05	0.10
Right posterior orbital gyrus	-1.57	0.12	0.19
Left posterior orbital gyrus	-3.12	0.002	**0.01**
Right planum polare	-2.95	0.003	**0.01**
Left planum polare	-3.43	0.001	**0.005**
Right precentral gyrus	-2.22	0.03	0.06
Left precentral gyrus	-2.21	0.03	0.06
Right planum temporale	0.42	0.67	0.77
Left planum temporale	-2.72	0.01	**0.02**
Right subcallosal area	1.43	0.15	0.23
Left subcallosal area	2.39	0.02	0.05
Right superior frontal gyrus	-2.43	0.02	**0.04**
Left superior frontal gyrus	-1.76	0.08	0.14
Right supplementary motor cortex	-0.14	0.89	0.93
Left supplementary motor cortex	-1.06	0.29	0.40
Right supramarginal gyrus	-0.48	0.63	0.73
Left supramarginal gyrus	-1.35	0.18	0.26
Right superior occipital gyrus	2.51	0.01	**0.04**
Left superior occipital gyrus	1.83	0.07	0.12
Right superior parietal lobule	-0.10	0.92	0.95
Left superior parietal lobule	-2.26	0.02	0.06
Right superior temporal gyrus	-2.41	0.02	**0.04**
Left superior temporal gyrus	-2.49	0.01	**0.04**
Right temporal pole	-6.57	1.01E-10	**1.47E-8**
Left temporal pole	-5.44	7.64E-8	**0.000002**
Right triangular part of the inferior frontal gyrus	-2.59	0.01	**0.03**
Left triangular part of the inferior frontal gyrus	-3.18	0.002	**0.01**
Right transverse temporal gyrus	-0.82	0.41	0.53
Left transverse temporal gyrus	-0.49	0.62	0.73

Supplementary References

Arnone, D., McKie, S., Elliott, R., Juhasz, G., Thomas, E. J., Downey, D., . . . Anderson, I. M. (2013). State-dependent changes in hippocampal grey matter in depression. *Mol Psychiatry, 18*(12), 1265-1272. doi:10.1038/mp.2012.150

Arnone, D., McKie, S., Elliott, R., Thomas, E. J., Downey, D., Juhasz, G., . . . Anderson, I. M. (2012). Increased amygdala responses to sad but not fearful faces in major depression: relation to mood state and pharmacological treatment. *Am J Psychiatry, 169*(8), 841-850. doi:10.1176/appi.ajp.2012.11121774

Dunlop, B. W., Binder, E. B., Cubells, J. F., Goodman, M. M., Kelley, M. E., Kinkead, B., . . . Mayberg, H. S. (2012). Predictors of remission in depression to individual and combined treatments (PReDICT): study protocol for a randomized controlled trial. *Trials, 13*, 106. doi:10.1186/1745-6215-13-106

Dutta, A., McKie, S., Downey, D., Thomas, E., Juhasz, G., Arnone, D., . . . Anderson, I. M. (2019). Regional default mode network connectivity in major depressive disorder: modulation by acute intravenous citalopram. *Transl Psychiatry, 9*(1), 116. doi:10.1038/s41398-019-0447-0

Ford, B. N., Yolken, R. H., Aupperle, R. L., Teague, T. K., Irwin, M. R., Paulus, M. P., & Savitz, J. (2019). Association of Early-Life Stress With Cytomegalovirus Infection in Adults With Major Depressive Disorder. *JAMA Psychiatry, 76*(5), 545-547. doi:10.1001/jamapsychiatry.2018.4543

Godlewska, B. R., Browning, M., Norbury, R., Igoumenou, A., Cowen, P. J., & Harmer, C. J. (2018). Predicting Treatment Response in Depression: The Role of Anterior Cingulate Cortex. *International Journal of Neuropsychopharmacology, 21*(11), 988-996. doi:10.1093/ijnp/pyy069

Godlewska, B. R., Hasselmann, H. W., Igoumenou, A., Norbury, R., & Cowen, P. J. (2014). Short-term escitalopram treatment and hippocampal volume. *Psychopharmacology (Berl), 231*(23), 4579-4581. doi:10.1007/s00213-014-3771-3

Green, S., Lambon Ralph, M. A., Moll, J., Deakin, J. F., & Zahn, R. (2012). Guilt-selective functional disconnection of anterior temporal and subgenual cortices in major depressive disorder. *Arch Gen Psychiatry, 69*(10), 1014-1021. doi:10.1001/archgenpsychiatry.2012.135

Habota, T., Sandu, A. L., Waiter, G. D., McNeil, C. J., Steele, J. D., Macfarlane, J. A., . . . McIntosh, A. M. (2019). Cohort profile for the STratifying Resilience and Depression Longitudinally (STRADL) study: A depression-focused investigation of Generation Scotland, using detailed clinical, cognitive, and neuroimaging assessments. *Wellcome Open Res, 4*, 185. doi:10.12688/wellcomeopenres.15538.2

Hamilton, M. (1960). A rating scale for depression. *J Neurol Neurosurg Psychiatry, 23*(1), 56-62. doi:10.1136/jnnp.23.1.56

Leucht, S., Fennema, H., Engel, R. R., Kaspers-Janssen, M., & Szegedi, A. (2018). Translating the HAM-D into the MADRS and vice versa with equipercentile linking. *J Affect Disord, 226*, 326-331. doi:10.1016/j.jad.2017.09.042

MacQueen, G. M., Hassel, S., Arnott, S. R., Jean, A., Bowie, C. R., Bray, S. L., . . . Kennedy, S. H. (2019). The Canadian Biomarker Integration Network in Depression (CAN-BIND): magnetic resonance imaging protocols. *J Psychiatry Neurosci, 44*(4), 223-236. doi:10.1503/jpn.180036

Misaki, M., Suzuki, H., Savitz, J., Drevets, W. C., & Bodurka, J. (2016). Individual Variations in Nucleus Accumbens Responses Associated with Major Depressive Disorder Symptoms. *Sci Rep, 6*, 21227. doi:10.1038/srep21227

Montgomery, S. A., & Asberg, M. (1979). A new depression scale designed to be sensitive to change. *Br J Psychiatry, 134*, 382-389. doi:10.1192/bjp.134.4.382

Nouretdinov, I., Costafreda, S. G., Gammerman, A., Chervonenkis, A., Vovk, V., Vapnik, V., & Fu, C. H. (2011). Machine learning classification with confidence: application of transductive conformal predictors to MRI-based diagnostic and prognostic markers in depression. *Neuroimage, 56*(2), 809-813. doi:10.1016/j.neuroimage.2010.05.023

Qiu, L., Xia, M., Cheng, B., Yuan, L., Kuang, W., Bi, F., . . . Gong, Q. (2018). Abnormal dynamic functional connectivity of amygdalar subregions in untreated patients with first-episode major depressive disorder. *J Psychiatry Neurosci, 43*(4), 262-272. doi:10.1503/jpn.170112

Rush, A. J., Trivedi, M. H., Ibrahim, H. M., Carmody, T. J., Arnow, B., Klein, D. N., . . . Keller, M. B. (2003). The 16-Item Quick Inventory of Depressive Symptomatology (QIDS), clinician rating (QIDS-C), and self-report (QIDS-SR): a psychometric evaluation in patients with chronic major depression. *Biol Psychiatry, 54*(5), 573-583. doi:10.1016/s0006-3223(02)01866-8

Sacchet, M. D., & Gotlib, I. H. (2017). Myelination of the brain in Major Depressive Disorder: An in vivo quantitative magnetic resonance imaging study. *Sci Rep, 7*(1), 2200. doi:10.1038/s41598-017-02062-y

Sacchet, M. D., Livermore, E. E., Iglesias, J. E., Glover, G. H., & Gotlib, I. H. (2015). Subcortical volumes differentiate Major Depressive Disorder, Bipolar Disorder, and remitted Major Depressive Disorder. *Journal of Psychiatric Research, 68*, 91-98. doi:https://doi.org/10.1016/j.jpsychires.2015.06.002

Sankar, A., Zhang, T., Gaonkar, B., Doshi, J., Erus, G., Costafreda, S. G., . . . Fu, C. H. (2016). Diagnostic potential of structural neuroimaging for depression from a multi-ethnic community sample. *BJPsych Open, 2*(4), 247-254. doi:10.1192/bjpo.bp.115.002493

Schwartz, J., Ordaz, S. J., Kircanski, K., Ho, T. C., Davis, E. G., Camacho, M. C., & Gotlib, I. H. (2019). Resting-state functional connectivity and inflexibility of daily emotions in major depression. *J Affect Disord, 249*, 26-34. doi:10.1016/j.jad.2019.01.040

Trivedi, M. H., McGrath, P. J., Fava, M., Parsey, R. V., Kurian, B. T., Phillips, M. L., . . . Weissman, M. M. (2016). Establishing moderators and biosignatures of antidepressant response in clinical care (EMBARC): Rationale and design. *Journal of Psychiatric Research, 78*, 11-23. doi:https://doi.org/10.1016/j.jpsychires.2016.03.001

Trivedi, M. H., Rush, A. J., Ibrahim, H. M., Carmody, T. J., Biggs, M. M., Suppes, T., . . . Kashner, T. M. (2004). The Inventory of Depressive Symptomatology, Clinician Rating (IDS-C) and Self-Report (IDS-SR), and the Quick Inventory of Depressive Symptomatology, Clinician Rating (QIDS-C) and Self-Report (QIDS-SR) in public sector patients with mood disorders: a psychometric evaluation. *Psychol Med, 34*(1), 73-82. doi:10.1017/s0033291703001107

Uher, R., Farmer, A., Maier, W., Rietschel, M., Hauser, J., Marusic, A., . . . Aitchison, K. J. (2008). Measuring depression: comparison and integration of three scales in the GENDEP study. *Psychol Med, 38*(2), 289-300. doi:10.1017/s0033291707001730

Wise, T., Marwood, L., Perkins, A. M., Herane-Vives, A., Joules, R., Lythgoe, D. J., . . . Arnone, D. (2017). Instability of default mode network connectivity in major depression: a two-sample confirmation study. *Transl Psychiatry, 7*(4), e1105. doi:10.1038/tp.2017.40

Wise, T., Marwood, L., Perkins, A. M., Herane-Vives, A., Williams, S. C. R., Young, A. H., . . . Arnone, D. (2018). A morphometric signature of depressive symptoms in unmedicated patients with mood disorders. *Acta Psychiatr Scand, 138*(1), 73-82. doi:10.1111/acps.12887

Zhao, Y., Niu, R., Lei, D., Shah, C., Xiao, Y., Zhang, W., . . . Gong, Q. (2020). Aberrant Gray Matter Networks in Non-comorbid Medication-Naive Patients With Major Depressive Disorder and Those With Social Anxiety Disorder. *Front Hum Neurosci, 14*, 172. doi:10.3389/fnhum.2020.00172

Zhao, Y., Zhang, F., Zhang, W., Chen, L., Chen, Z., Lui, S., & Gong, Q. (2021). Decoupling of Gray and White Matter Functional Networks in Medication-Naïve Patients With Major Depressive Disorder. *J Magn Reson Imaging, 53*(3), 742-752. doi:10.1002/jmri.27392

Zheng, H., Ford, B. N., Bergamino, M., Kuplicki, R., Hunt, P. W., Bodurka, J., . . . Savitz, J. (2021). A hidden menace? Cytomegalovirus infection is associated with reduced cortical gray matter volume in major depressive disorder. *Mol Psychiatry, 26*(8), 4234-4244. doi:10.1038/s41380-020-00932-y